

# BANDED WAVEGUIDES: TOWARDS PHYSICAL MODELING OF BOWED BAR PERCUSSION INSTRUMENTS

*Georg Essl*

*Perry R. Cook*

Computer Science Department  
Princeton University  
08544 Princeton, New Jersey, U.S.A.  
gessler@cs.princeton.edu

Computer Science Department (also Music)  
Princeton University  
08544 Princeton, New Jersey, U.S.A.  
prc@cs.princeton.edu

## ABSTRACT

Efficient physical models of bar percussion instruments which preserve spatial sampling are not yet available. In this paper, *banded waveguides* are proposed as an efficient method for simulating the physics of bars including spatial sampling. In addition two other models are investigated. One is a generalization of the waveguide idea replacing unit delays by all-pass filters modeling the phase delay characteristics. The other extends on existing finite difference (FD) methods. According to this study all-pass filter chains show no advantages over FDs in terms of performance and physical realism. Finally, real bars were the target of experimental measurements.

## 1. INTRODUCTION

Recently the technique of bowing bar percussion instruments has become popular among composers and percussionists. However, sound generation in these systems has not yet been studied. Existing physical models with computational efficiency [1, 2, 3, 4] model only the modes of the bar and hence remove spatial sampling. In order to interface with a non-linearly coupled excitation, the physical quantities at spatial points are necessary inputs to the non-linearity.

While there is no previous work on the bowed bar, the bowed string has been intensively studied [5, 6] and physical modeling has been successfully applied to the problem [7]. The concept of digital waveguide filters [8] has led to models which are efficient enough to be used in performance. The struck bar has been modeled either using sinusoidal [1, 2] or modal [3, 4] methods for efficient computation or by finite difference methods [9] if high accuracy is desired or transient behavior is of interest.

In the work described here the mechanism behind the bow-bar interaction is investigated. In particular there is interest in creating a computer-simulated physical model for the purpose of supporting the theoretical understanding. Also, a computationally efficient physical model is sought for use in musical performance, which allows general (i.e. linear and nonlinear) spatially localized physical excitations. In the following sections the physics of bars is briefly reviewed, the issue of modeling the system is discussed, and then measurements of bowed and struck bars are reported.

## 2. PHYSICS OF BARS

Transverse vibration of bars is well described by the 1-D Euler-Bernoulli-model [10], given that the bar is thin compared to its length and the exact frequencies of very high order partials is not important:

$$\frac{\partial^2}{\partial x^2} \left( EI \frac{\partial^2 y}{\partial x^2} \right) + \rho A \frac{\partial^2 y}{\partial t^2} = f(x, t) \quad (1)$$

$EI$  is the flexural rigidity ( $E$  being Young's modulus and  $I$  being the cross-sectional moment of inertia) and  $\rho A$  is the mass term ( $\rho$  being mass density per unit length and  $A$  being the cross-sectional area). In general these quantities are not constants but may depend on  $x$ .  $f(x, t)$  is an externally applied transverse force on the bar. In order to model friction additional terms have to be added (see [9]). If cross section and elasticity properties are uniform, (1) becomes a linear 4th order partial differential equation which lends itself easily to analytical solution. In particular, when inserting the solution of a single frequency  $y = Y(x)e^{j\omega t}$  the wave velocity can be calculated from (1) with  $f(x, t) = 0$  letting  $a = \sqrt{EI/\rho A}$ :

$$v = \sqrt{a\omega} \quad (2)$$

The wave velocity depends on the frequency of the traveling wave and hence arbitrary wave shapes disperse as higher frequencies propagate faster than lower ones. The general solution of (1) for constant coefficients and in the absence of an external force can be derived to be [10]:

$$y = e^{j\omega t} (Ae^{kx} + Be^{-kx} + Ce^{jkx} + De^{-jkx}) \quad (3)$$

The first two terms are stationary oscillations (the so-called "near-field" terms) and the second two terms are left- and right-going propagation terms. The constants  $A$ ,  $B$ ,  $C$  and  $D$  depend on the particular boundary conditions. The "free-free" boundary condition, as is typical for bars in musical instruments, yields the well-known stretched and inharmonic partials of a uniform bar (1 : 2.756 : 5.404 : 8.933 : ...) as heard from glockenspiels. Marimba, xylophone and vibraphone bars are undercut, stretching the partials into harmonic ratios of either 1 : 4 : 10 or 1 : 3 : 6.

### 3. PHYSICAL MODELING OF BARS

In the literature, the struck bar has been modeled either using sinusoidal modeling, modal filter synthesis, or finite difference/element methods. Sinusoidal and modal filtering methods are efficient. The eigenmodes are directly modeled, but spatial sampling of the bar is lost. Even though the modeling of the behavior of spatially different excitations is possible for struck excitations, where the produced oscillations are free, it is not clear how the problem of interfacing a non-linear bow interaction at a spatial point with a modal synthesis model can be solved. Finite difference and finite element methods are not efficient, yet these preserve spatial sampling. By discretizing the solution of the Euler-Bernoulli equation, two models are investigated in order to arrive at a physical model which achieves both spatial sampling and efficient computation.

#### 3.1. Generalized Waveguide Model

The generalized waveguide is the discretization of the propagation terms of equation (3). As can be seen from equation (2), the phase velocity depends on the frequency. Starting from the picture of the usual waveguide, the unit delays are replaced by frequency dependent delays as symbolically depicted in figure 1.  $R$  is the appropriate reflection-function at the boundary.

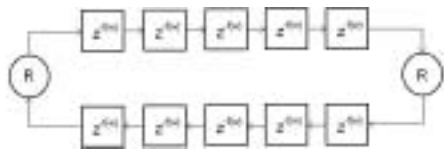


Figure 1: *Generalized Waveguide: Waveguide with frequency-dependent phase delay.*

If losses are modeled separately, the frequency dependent delays are all-pass filters with an appropriately modeled phase delay response. This has strong connections to and is strongly motivated by work on modeling the stiffness of strings starting from a mixed bar/string-equation using all-passes [11, 12, 13, 14]. These references discuss details of the all-pass design. While, depending on the order of the all-passes used, good approximation to the phase delay characteristics of bars can be achieved, this approach shows poor performance. The number of all-passes needed depends on the fundamental frequency of the bar. It was found that for the same spatial and temporal sampling, 10th order all-pass chains require more computation than an implicit finite difference method implementation (after [9]). This performance comparison matches the counted number of floating-point multiplications and additions as found in the all-passes and the band-diagonal solver used in the finite difference implementation. While this model preserves spatial sampling and hence would allow for non-linear spatially localized interactions, it is neither use-

ful for musical performance nor advisable for acoustical modeling purposes, because finite differencing also models the near-field terms.

#### 3.2. The Banded Waveguide Model

A lesson learned from generalized waveguides is that attempting to closely approximate the phase delay characteristics is costly. One can take two views in motivating the idea of banded waveguides:

(1) Discretization view: the phase delay characteristics are approximated by a less accurate model. This can be achieved by quantizing the phase delay characteristics. This frequency quantization is a second quantization introduced in addition to the spatial/temporal quantization. (2) Physical view: model the system by modeling propagation of the wave train closures which would then result in the correct system modes. Natural vibrations (modes) occur if the wave train closes on itself after one round trip [10]. If that's not the case the corresponding frequency component is damped by destructive interference.

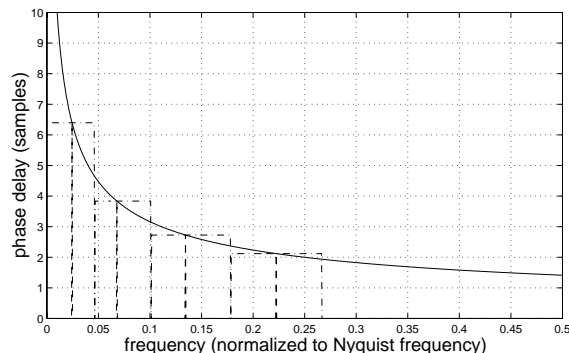


Figure 2: *Quantization of phase delay characteristics.*

A flat quantization over a region in the phase response (see figure 2) makes the phase delay constant in that region which can be cheaply modeled using a standard waveguide filter. However, only frequencies in the corresponding band should enter the waveguide. Hence an additional bandpass filter is required. If the loop delay is tuned to a mode of the system, this corresponds to an exact simulation of the wave train closure and approximation in the neighborhood of that mode. To avoid large errors in this neighborhood approximation, the higher harmonic resonances of the waveguide should not be within the modeled frequency band.

Figure 3 shows the structure of a single banded waveguide and the frequency characteristic. The dashed curve is an ideal bandpass filter response which windows the desired frequency band. The dash-dotted curve depicts a low-Q biquad filter response used as a bandpass filter approximation. A complete system can be assembled by taking multiple banded waveguide structures, tuned to the respective modes they model. In the absence of nonlinearities each banded waveguide is com-

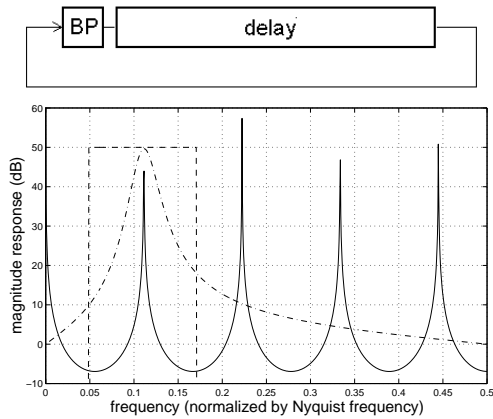


Figure 3: A banded waveguide (top) and its spectrum.

pletely decoupled from all other ones. If the sampling rates of all banded waveguides are the same, then they will be of different lengths even though they are representing modes in a single bar. Hence dependent on the mode, the spatial sampling is different for each frequency band. If the spatial sampling is uniform, the sampling rate for each banded waveguide must be different. This multi-resolution is the result of the sampling in both the time and the frequency domain. Pickup points and points of excitation hence have to be located in the banded waveguides using the phase velocity (equation (2)). Fractions in the spatial sampling can be dealt with in the same way as for ordinary waveguides. The physical quantity can be calculated as the sum of all left- and right-going contributions of all waveguides.

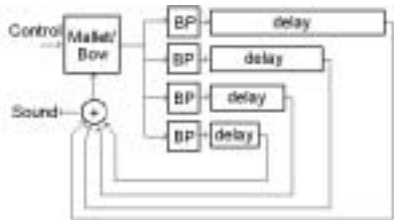


Figure 4: A simplified banded waveguide model.

Figure 4 depicts a simplified version of a banded waveguide implementation of a bar using four modes. This system embodies a hybrid model of modal filter and waveguide synthesis. The “modal” filters are however more broadband instead of high-Q in order to achieve a sampling of the phase-delay characteristics. The actual resonance behavior is modeled by the waveguide. Low-Q biquad filters were used as bandpass filters. It should be noted that this approach would allow for high-order approximations to the ideal bandpass or even to filters which more closely approximate the progression of the phase delay characteristic in each band, but this would lead to the loss of computational efficiency on current systems. It should be noted that the computational complexity of banded waveguides

for a fixed number of modeled modes is independent of the length (thus pitch) of the bar, whereas this is not the case for generalized waveguides, FDE and FEM.

#### 4. MEASUREMENTS OF REAL BARS

Striking and bowing measurements were performed on two aluminum vibraphone bars (low and medium register), one medium register wooden xylophone bar, a uniform wooden bar and a uniform thin bar of aluminum. Impulse response and reference spectrum measurements were performed using a force hammer. The impulse responses of uniform bars show the characteristic inharmonic partials in good agreement with theory. The impulse responses of the tuned bars reveal the usual double octave tuning 1 : 4. The tuning of the third partial is only reasonably accurate for the low register vibraphone bar. All other tuned bars have inharmonic third partials at a ratio of less than 1 : 10.

The bowing measurements were performed using a double-bass bow machine consists of a motor-driven rubber wheel 3cm wide and with a diameter of 5cm. A band of horse hair is wound around the wheel once, glued, and pressed flat. In hand-bowing, constancy of velocity and force cannot be guaranteed and the data is more approximate. Hand-bowing and the bowing machine were used to measure the spectral content and form of the partials when bowed, dependency of amplitude on velocity (assuming constant force), dependency of amplitude and spectral content on force (assuming constant velocity), and regions of oscillation depending on velocity and force. Measuring the vibrational shape by high-speed photography indicates an upper bound of the vibrational amplitude. The mea-

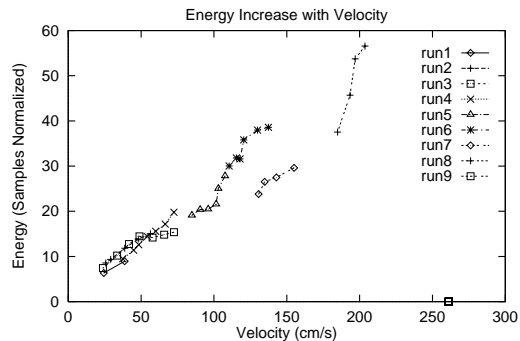


Figure 5: Energy response with increasing velocity.

surements reveal that the amplitude of the steady-state oscillation of the system increases with velocity (figure 5), whereas it is unaffected by variations in force. The initial transient and the spectral content, however, do increase with force. The regime of oscillation is found to depend on both bowing velocity and bowing force. In general, minimum and maximum bowing velocity increases with increasing bowing force. All the results mentioned so far correspond to measured results known from the bowed string[5, 6]. However,

it should be pointed out that the usual intuition used for the bowed string derived from Helmholtz motion to understand the behavior regarding minimum and maximum bowing force, force dependent spectral content from “corner rounding and sharpening” cannot be applied to the bowed bar. This is due to the fact that the bar is strongly dispersive, unlike the weak stiffness of violin strings, thus Helmholtz motion cannot be assumed. The effect of near-fields remains an open question and there is evidence in measurements at high speeds with the bowing machine that the near-fields at the free boundaries contribute significantly to the oscillation. Also in the bowed string case, a harmonic spectrum for both the free oscillation and the steady-state oscillation of a bow excitation is observed. This allowed Helmholtz to treat the problem analytically as free oscillation, even though it was found later that the free oscillation treatment is not exactly valid. The spectra of bowed uniform and nonuniform bars show a harmonic spectrum with the amplitude of the partials dependent on the vicinity of an eigenfrequency of the bar. This is to be expected from forced oscillation systems [10].

## 5. PHYSICAL MODELING OF THE BOW-BAR INTERACTION

Simulated models of the bow-bar interaction have been added to an existing implicit finite difference approach [9] using both a dynamic (stick-slip) as well as a simplified forced oscillation approach. Sustained oscillations were achieved in both cases. In particular the forced oscillation spectrum, minimum bowing force, and velocity dependent amplitude have been reproduced by these simulations. Also the banded waveguide model for bowing was implemented following the scattering view known from waveguide based bowed string models [15]. This model properly captures the behavior of minimum and maximum bowing force and velocity. The spectrum shows the characteristic harmonic forced oscillation spectrum (figure 6). It should be noted that

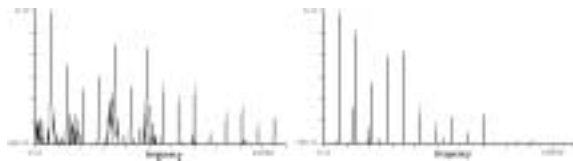


Figure 6: *Spectra of real and simulated bowed bar.*

in this simulation the steady state oscillation tends to lock to higher modes of the bar. This phenomenon can be observed experimentally when bowing a low register bar in the middle. The nature of this mode locking is not yet well understood.

## Acknowledgments

Georg Essl would like to thank the Austrian Federal Ministry for Science and Traffic for financial support. This work was supported by Intel, Interval Research, and the Arial Foundation.

## 6. REFERENCES

- [1] Serra, X., “A Computer Model for Bar Percussion Instruments,” Proc. ICMC’86, 257–262, 1986.
- [2] van den Doel, K., Pai, D., “The Sound of Physical Shapes,” Tech. Report 96-03, Dept. of Computer Science, University of British Columbia, Canada, 1996.
- [3] Wawrzynek, J., “VLSI Models for Sound Synthesis,” In Mathews, M., Pierce, J., eds., “Current Directions in Computer Music Research,” MIT Press, 1989.
- [4] Cook, P., “Physically Informed Sonic Modeling (PhISM): Synthesis of Percussive Sounds,” CMJ 21:3, 38–49, 1997.
- [5] Cremer, L., “The Physics of the Violin,” MIT Press, 1984.
- [6] Hutchins, C., Benade, V., eds., “Research Papers in Violin Acoustics 1975-1993,” Acoustical Society of America, 1997.
- [7] Woodhouse, J., “Physical Modeling of Bowed Strings,” CMJ 16:4, 43–56, 1992 and references therein, especially McIntyre, M., Woodhouse, J., “On the Fundamentals of Bowed-String Dynamics,” Acustica 43:2, 93–108, 1979, reprinted in [6].
- [8] Smith, J., “Physical Modeling using Digital Waveguides,” CMJ 16:4, 74-91, 1992.
- [9] Chaigne, A., Doutaut, V., “Numerical simulation of xylophones. I. Time-domain modeling of the vibrating bars,” J. Acoust. Soc. Am. 101:1, 539-557, 1997 and Doutaut, V., Maignon, D., Chaigne, A., “Numerical simulations of xylophones. II. Time-domain modeling of the resonator and of the radiated sound pressure,” J. Acoust. Soc. Am. 103:3, 1633-1647, 1998.
- [10] Cremer, L., Heckl, M., Ungar, E., “Structure-Borne Sound,” 2nd edition, Springer Verlag, 1988.
- [11] Jaffe, D., Smith, J., “Extension of the Karplus-Strong plucked string algorithm,” CMJ 7:2, 43-45, 1983.
- [12] Paladin, A., Rocchesso, D., “A Dispersive Resonator in Real Time on MARS Workstation,” Proc. ICMC’92, 146-149, 1992.
- [13] van Duyne, S., Smith, J., “A Simplified Approach to Modeling Dispersion Caused by Stiffness in Strings and Plates,” Proc. ICMC’94, 407-410, 1994.
- [14] Rocchesso, D., Scalcon, F., “Accurate Dispersion Simulation for Piano Strings,” Proc. Nordic Acoustical Meeting’96, 407-414, 1996.
- [15] Smith, J., “Efficient Simulation of the Reed-Bore and Bow-String Mechanisms,” Proc. ICMC, 275–280, 1986.